

## A PILOT STUDY

# Noninvasive study of brain tumours metabolism using phosphorus-31 magnetic resonance spectroscopy

Hnilicova P<sup>1</sup>, Richteroval R<sup>2</sup>, Zelenak K<sup>3</sup>, Kolarovszki B<sup>2</sup>, Majercikova Z<sup>4</sup>, Hatok J<sup>4</sup>*Biomedical Centre Martin, Jessenius Faculty of Medicine in Martin, Comenius University in Bratislava, Martin, Slovakia. [petra.hnilicova@uniba.sk](mailto:petra.hnilicova@uniba.sk)***ABSTRACT**

Phosphorus-31 magnetic resonance spectroscopy (<sup>31</sup>P MRS) is currently not accepted as a diagnostic tool in the neuro-oncological practice, although it provides useful non-invasive information about biochemical processes ongoing in the intracranial tumours. This pilot study was aimed to present the diagnostic capability of the <sup>31</sup>P MRS in brain tumour examination, even its application on clinical 1.5T MR scanner.

Seven patients with brain tumorous lesions (four glioblastomas, one ependymoma, and two lung metastasis) underwent multivoxel *in vivo* <sup>31</sup>P MRS performed on clinical 1.5 T MR scanner within measurement time of 20 minutes. Comparing two selected voxels, one in the tumour and the other one in the normal-appearing brain tissue, enabled to investigate their metabolic differences. Enhanced markers of membrane phospholipids synthesis (significantly increased phosphomonoesters ratios) than markers of their degradation (significantly decreased phosphodiester ratios) manifested a higher cell proliferation ongoing in tumours. High energetic tumorous tissue demands leading to anaerobic metabolic turnover were present as a significant decline in phosphocreatine ratios and adenosine triphosphates. Intracellular pH evaluation showed a tumorous tendency to alkalize.

<sup>31</sup>P MRS enables the non-invasive metabolic characterization of intracranial tumours and thus appears to be a clinically useful method for the determination of ongoing tumour pathomechanisms (Fig. 2, Ref. 26). Text in PDF [www.elis.sk](http://www.elis.sk)

KEY WORDS: brain tumour, <sup>31</sup>P MRS, 1.5 Tesla; energetic metabolism.

**Introduction**

Phosphorus-31 MR Spectroscopy (<sup>31</sup>P MRS) is a very useful clinical tool with great potential mostly in neuro-oncological practice, because it provides non-invasive insight into the composition of the examined tissue *in vivo*, and allows to obtain information about cellular energy or membrane metabolism (1, 2). <sup>31</sup>P MRS enables direct measurement of energy metabolites like phosphocreatine (PCr), adenosine-triphosphates (ATP), inorganic phosphate (Pi), as well as and indirectly evaluate intracellular pH

and cell membrane phospholipids composition through phosphomonoesters (PME), and phosphodiester (PDE) (1, 3). Although it can be demonstrated that different concentrations of various phosphorus metabolites measured spectroscopically between the brain tumours and normal brain tissue (3, 4, 5), the clinical application of <sup>31</sup>P MRS for the examination of brain tumours has limitations, until recently (1, 2, 6). One reason for this may be the relatively low sensitivity of <sup>31</sup>P MRS at 1.5 T field strength (1, 7). Therefore, the longer scan time or larger single-voxels had to be chosen (~ 40–100 cc), making it impossible to study heterogeneity of the intracranial tumours (4, 8, 9). In this pilot study, the <sup>31</sup>P MRS signal was obtained using the multivoxel technique with relatively small voxel volume (~ 27 cm<sup>3</sup>) and in a tolerable scan time of 20 minutes, including the scanning for localization. This pilot study aimed to achieve clinically feasible <sup>31</sup>P MRS brain tumours examination, despite application on basic clinical 1.5 T MR scanner, showed the medical relevance of non-invasive metabolic characterization of intracranial tumours and investigated the most useful <sup>31</sup>P MRS parameters, which may determinate the ongoing tumour pathomechanisms.

**Materials and methods***Study participants*

All examinations of this <sup>31</sup>P MRS pilot study were carried out in compliance with the local institutional medical ethics com-

<sup>1</sup>Biomedical Centre Martin, Jessenius Faculty of Medicine in Martin, Comenius University in Bratislava, Martin, Slovakia, <sup>2</sup>Clinic of Neurosurgery, Jessenius Faculty of Medicine in Martin, Comenius University in Bratislava, Martin, Slovakia, <sup>3</sup>Clinic of Radiology, Jessenius Faculty of Medicine in Martin, Comenius University in Bratislava, Martin, Slovakia, and <sup>4</sup>Department of Medical Biochemistry, Jessenius Faculty of Medicine in Martin, Comenius University in Bratislava, Martin, Slovakia

**Address for correspondence:** P. Hnilicova, Ing, PhD, Biomedical Centre Martin, Jessenius Faculty of Medicine in Martin, Comenius University in Bratislava, Mala Hora 4D, SK-036 01 Martin, Slovakia.  
Phone: +421.43.2633 660

**Acknowledgments:** This work was supported by the Slovak Research and Development Agency under Contract No. APVV-18-0088 and by the project implementation: "Centre of Excellence for Research in Personalized Therapy (Cevypet)," Itms: 26220120053 supported by the Operational Programme Research and Innovation funded by the ERDF.

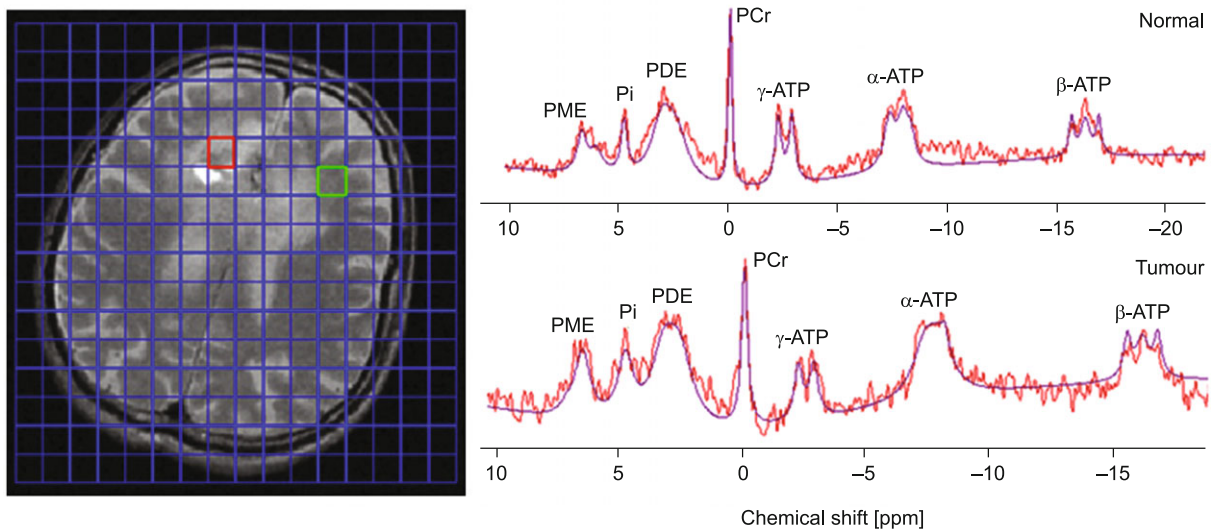


**Fig. 1.**  $^{31}\text{P}$  MRS of the tumorous and normal-appearing brain tissue. For all participants, one voxel in the tumour (red voxel) and another one in normal-appearing brain tissue (green voxel) were chosen, and  $^{31}\text{P}$  MR spectra were evaluated in jMRUI. In fitted spectra measured on 1.5T are detectable peaks of phosphomonoesters (PME), phosphodiester (PDE), adenosine triphosphates ( $\alpha$ - $\beta$ - $\gamma$ -ATP), phosphocreatine (PCr), and inorganic phosphate (Pi).

mittee and after obtaining a written informed consent from study participants. In the study, seven patients were enrolled (the mean age:  $65 \pm 12$  years; 3 males and 4 females), who had suspected brain tumour lesions detected during the standard clinical MRI examination. All the patients underwent  $^{31}\text{P}$  MRS before any of the surgical nor therapeutic treatment procedures. After a subsequent histological analysis, four grade IV glioblastomas, one grade III ependymomas, and two metastasis of lung carcinoma were confirmed.

#### Data measurement and analysis

All measurements were performed on a clinical 1.5 T MR scanner Siemens Magnetom Symphony (Siemens, Erlangen, Germany) using the  $^{31}\text{P}$  quadrature volume head coil (Stark contrast, Erlangen, Germany) operating at 25.7 MHz for  $^{31}\text{P}$ -signal detection. The whole examination protocol was in total duration of 20 min and consisted of multi-slice  $T_2$ -weighted MRI (2D spin multi-echo, 24 slices with a 3.5 mm slice thickness and 5 mm interslice gap,  $245 \times 280 \text{ mm}^2$  field of view, repetition time TR/echo time TE = 3000/51 ms) and  $^{31}\text{P}$  MRS. For multivoxel spectroscopy, the 3D free induction decay (FID) chemical shift imaging (CSI) sequence was carried out in an axial plane with the following parameters: TR/TE = 290/2.3 ms, CSI grid  $8 \times 8 \times 8$  interpolated to  $16 \times 16 \times 16$ , nominal voxel size  $32.5 \times 32.5 \times 32.5 \text{ mm}^3$ . All spectroscopic data were evaluated in jMRUI 5.0 software (10). The software allows for overlapping the  $T_2$ -weighted MRI with the spectroscopic grid, enabled to select voxels in the desired tissue area. For each of study participants, one voxel inside the tumour and one voxel in normal-appearing brain tissue (contralaterally to the tumour voxel) were selected (Fig. 1). For data quantification, a priori information files were entered, which were implemented into the AMARES evaluation algorithm (10). After zero-filling

(4096 points) and 5 Hz exponential line broadening, the  $^{31}\text{P}$  MR spectra were obtained (Fig. 1). The integrals of measured  $^{31}\text{P}$  metabolites were evaluated, and the following ratios were calculated: PCr/Pi, PCr/ATP, Pi/ATP, PME/PDE, PME/PCr, PME/Pi, PME/ATP, PDE/PCr, PDE/Pi, and PDE/ATP. The intracellular pH of the examined tissue was calculated by using the chemical shift of Pi relative to the PCr peak (10, 11).

#### Statistics

The mean values of the intracellular pH and metabolite ratios between the normal-appearing brain tissue group (normal) and the brain tumours group (tumour) were compared by using the two-tailed paired t-test. p value of less than 0.05 was considered significant. The statistical analysis was performed by using the SPSS v.15.0 software package (Chicago, IL, USA).

#### Results

Comparing  $^{31}\text{P}$  MRS metabolite ratios and pH in the tumour and in the normal-appearing brain tissue (Fig. 2), proved metabolic differences of these groups. In tumorous tissue, significantly increased phosphomonoesters ratios (PME/PDE, PME/PCr, PME/Pi, and PME/ATP) and significantly decreased phosphodiester ratios (PDE/PCr, PDE/Pi, and PDE/ATP) was observed. Furthermore, a significant decline in PCr/Pi and PCr/ATP ratios and a significant increase in Pi/ATP were shown, compared to the normal-appearing brain tissue. The intracellular pH in the brain tumours tended towards alkalization. The highest differences between tumorous and normal brain tissue reflected PME/PDE ( $p < 0.001$ ), followed by PME/PCr with PME/ATP ( $p = 0.001$ ;  $p = 0.007$ ), and PCr/Pi ( $p = 0.010$ ) ratios (Fig. 2).

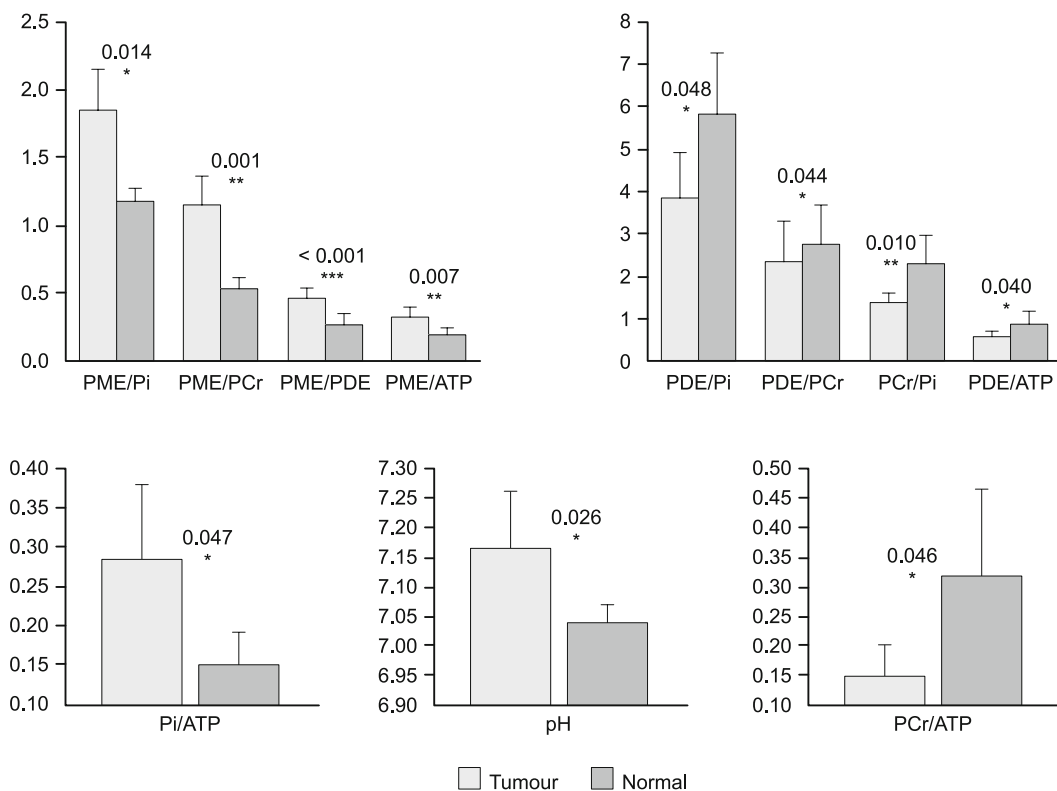


**Fig. 2. Differences between tumorous and normal brain tissue based on  $^{31}\text{P}$  MRS. Visualization of differences between tumours (tumour) and normal-appearing brain tissue (normal) among all  $^{31}\text{P}$  MRS metabolite ratios and pH. The statistical significance of these differences was depicted as follows: \* significant ( $0.01 \leq p < 0.05$ ), \*\* very significant ( $0.001 \leq p < 0.01$ ), and \*\*\* extremely significant ( $p < 0.001$ ).**

Abbreviations: PME = phosphomonoesters, PDE = phosphodiester, PCr = phosphocreatine, ATP = adenosine triphosphates, Pi = inorganic phosphate.

## Discussion

The multivoxel  $^{31}\text{P}$  MRS examination implemented under the basic clinical condition on 1.5 T magnetic field strength combined with semi-automatic data quantification in jMRUI provides a straightforward method for spatial-mapping of  $^{31}\text{P}$ -containing metabolite ratios across the brain. Similar  $^1\text{H}$  MRS metabolite mapping of intracranial tumours has been previously studied in our group (12), showing a clinical utility to extend the palette of detected metabolites for comprehensive non-invasive tumorous tissue characterization. Using  $^{31}\text{P}$  MRS enables to provide information about the energetic and phospholipid metabolism or intracellular pH, as was previously declared (4,5,9). Although the most useful  $^{31}\text{P}$ -metabolite marker for clinical oncology was not agreed yet (1, 4, 6).

### Membrane phospholipids metabolism

Cell membranes, especially membrane phospholipids, which are involved in membrane structure, signal transduction mechanisms, regulation of cell proliferation, and lipoprotein metabolism are important for tumorigenesis (13, 14). Although it is not feasible to directly measure membrane phospholipids due to their fixed membrane integration, using  $^{31}\text{P}$  MRS is possible to detect phospholipids precursors as well as their degradation products (15,

16). Furthermore, the basic clinical 1.5 T field strength limits the  $^{31}\text{P}$  MRS detection and thus enables to evaluate only the joined PME-signal consisting mainly of phosphocholine with phosphoethanolamine and joined PDE-signal composed of glycerophosphocholine and glycerophosphoethanolamine (1, 5, 16). Nevertheless, both PME, as well as PDE, are considered as markers for tumour detection (1, 4, 5). In our study, a significant elevation in all evaluated PME ratios (PME/PCr, PME/Pi and PME/ATP) as well as in PME/PDE ratio in tumours compared to that in the normal-appearing brain tissue was observed. On contrary, all PDE ratios (PDE/PCr, PDE/Pi, and PDE/ATP) were significantly decreased in tumours. Considering elevated PME ratios as a marker of membrane synthesis (4, 9, 17) combined with the decline in PDE ratios as an indicator of membrane catabolism (1, 5, 18), the tumorous tissue examined in our study manifested a shift toward membrane synthesis and tumour growth. According to another experimental tumour studies, an increase of the PME is related to malignant progression, relapses, and increasing grade of tumour malignancy, and the significant increase in the PDE may indicate therapy-induced membrane degradation in dying cells (4, 17, 18). However, a typical feature of phosphorus spectra of proliferating intracranial tumours are predominant PME peaks, but contrary to healthy tissue, also increased values of PDE peaks as the result of the overall metabolism of higher cellular density (1, 5, 9). There-

fore, the ratio of PME/PDE can serve as an index of the metabolism of membrane phospholipid and reflect changes in the rate of membrane synthesis or metabolic turnover (1, 9, 16).

#### Cellular energy metabolism

Cellular energy metabolism is a crucial determinant of cell proliferation or cell death (5, 14). Therefore,  $^{31}\text{P}$  MRS is regarded as a useful clinical application enabling the non-invasive disclosure of cells energetic processes through ATP, PCr, and Pi, compounds that are metabolically interconnected (14, 19, 20). ATP hydrolysis is the reaction, by which chemical energy from the high-energy phosphoanhydridic bonds in ATP is released, and by which the Pi and ADP are formed (19, 21). Whereas this energy is utilized for most cellular processes and functions (14, 21, 22), ATP is considered as a marker of the momentary energetic state of the cell (1, 22). The metabolic pathways of ATP and PCr are tightly coupled via the enzyme creatine kinase that generates ATP by the transfer of a phosphate group from PCr to ADP under conditions of higher energy demands and/or insufficient ATP production through oxidative phosphorylation in the cellular mitochondria (20, 21, 23). Although the PCr is in the brain tissue under physiological condition stable, it is rapidly utilized for fast ATP recovery in the case of energetic needs (1, 19, 22). Therefore, PCr is considered as a sensitive marker for mitochondrial efficiency. Its decline usually suggests a mitochondrial dysfunction and/or tissue excessive requirements (5, 14, 23). Under physiological brain cell conditions, the majority of glucose is metabolized oxidatively, leading to a stable PCr-ATP-Pi chemical exchange system (13, 14, 21). But tumour cells have a higher demand for metabolic energy than normal cells (4, 5, 9). Nevertheless, they rely mostly on anaerobic glycolysis (Warburg effect) even in the presence of adequate oxygen supply (21, 22). Tumour cells meet their increased demand for ATP by increasing glucose transport into the cells and by the acceleration of glycolysis (14, 21, 23). Recent studies of metabolic pathways showed that in the presence of abundant nutrients, anaerobic glycolysis could potentially produce ATP in greater amounts and faster than mitochondrial oxidative phosphorylation (21, 23). In this pilot study of brain tumours, the PCr/Pi and PCr/ATP ratios were significantly reduced, while the Pi/ATP ratio was elevated compared to the normal-appearing brain tissue. These results indicated increased values of ATP, as well as Pi levels and contrary, decreased PCr values in tumorous tissue, demonstrating high energetic demands and mitochondrial inefficiency, leading to an anaerobic metabolic turnover. Our findings were consistent with several other studies that reported that high energy demand in the brain tumours required correspondingly high rates of ATP production, but also ATP utilization, leading to energy-source reservoir dephosphorylation (PCr decline) together with a higher ATP-production as well as its consumption (Pi increment) (1, 4, 19, 22). Besides, an increased Pi was associated with a dysfunction of the respiratory chain, which is a hallmark of tissue hypoxia (5, 9, 13).

#### Intracellular pH

Intracellular pH could be possibly non-invasively evaluated using  $^{31}\text{P}$  MRS based on the chemical shift of endogenous Pi (1,

11). The Pi position is determined by its form of conjugated pair of anions  $\text{H}_2\text{PO}_4^-$  and  $\text{HPO}_4^{2-}$ , which change rapidly depending on the dissociation reactions (4, 24). Despite the assumption that tumour cells have acidic metabolism due to an increased lactate production, measurements of intracellular tumours pH by  $^{31}\text{P}$  MRS reported more alkaline values (11, 22, 25). In this pilot study, a tendency of tumour alkalization ( $\text{pH} = 7.16 \pm 0.1$ ) compared to normal-appearing brain tissue ( $\text{pH} = 7.04 \pm 0.03$ ) was also observed. Several studies reported intracellular pH in the healthy human brain in the range of 7.01–7.07 (4, 9, 25). Furthermore, in intracranial tumours it was previously described that solid tumorous part was alkaline ( $\text{pH} = 7.15\text{--}7.48$ ), contrary to the acidic ( $\text{pH} = 6.45\text{--}6.87$ ) extracellular tumour environment (9, 25, 26). It may be explained by the function of tumour cells to export the excessive lactate along with protons via cell-specific monocarboxylate transporters instead of utilizing it as a nutrient (13, 14, 26). Besides, in tumour cells, an enhanced activity of  $\text{H}^+$  extruding pathways was found, like the  $\text{Na}^+/\text{H}^+$  exchanger or by buffering intracellular protons via the transmembrane carbonic anhydrases, both counteracting the intracellular proton accumulation (15, 22). Consequently, the extracellular environment gets more acidic, enhancing the invasiveness of tumour cells, and promoting angiogenesis (21, 23).

#### Conclusion

This pilot study declared the usefulness of multivoxel  $^{31}\text{P}$  MRS examination applied under the basic 1.5 T field strength as a clinically feasible method for  $^{31}\text{P}$ -containing metabolite mapping across the brain and thus a useful diagnostic tool enabling tumorous tissue characterization. From all investigated parameters, the PME (mostly PME/PDE), followed by PCr/Pi ratios seems to be the most useful markers for the detection of the brain tumorous tissue.

#### References

1. Wijnen JP. Multi-nuclear magnetic resonance spectroscopy of human brain tumours: Radboud University Nijmegen 2010; 193.
2. Faghihi R, Zeinali-Rafsanjani B, Mosleh-Shirazi MA et al. Magnetic Resonance Spectroscopy and its Clinical Applications: A Review. *J Med Imaging Radiation Sci* 2017; 48: 233–253.
3. Peeters TH, van Uden MJ, Rijpmma A, Scheenen TWJ, Heerschap A. 3D  $^{31}\text{P}$  MR spectroscopic imaging of the human brain at 3 T with a  $^{31}\text{P}$  receive array: An assessment of  $^1\text{H}$  decoupling, relaxation times,  $^1\text{H}$ - $^{31}\text{P}$  nuclear Overhauser effects and  $\text{NAD}^+$ . *NMR in Biomedicine*. 2019; e4169.
4. Ha DH, Choi S, Oh JY, Yoon SK, Kang MJ, Kim KU. Application of  $^{31}\text{P}$  MR Spectroscopy to the Brain Tumors. *Korean J Radiol* 2013; 14 (3): 477–486.
5. Solivera J, Cerdán S, Pascual JM, Barrios L, Roda JM. Assessment of  $^{31}\text{P}$ -NMR analysis of phospholipid profiles for potential differential diagnosis of human cerebral tumors. *NMR Biomed* 2009; 22 (6): 663–74.
6. Barker PB. *Clinical MR Neuroimaging: Physiological and Functional Techniques*. 2nd ed. Cambridge (UK): Cambridge University Press; Chapter 1, Fundamentals of MR spectroscopy 2010; 5–20.
7. Novak J, Wilson M, MacPherson L, Arvanitis TN, Davies NP, Peeta AC. Clinical protocols for  $^{31}\text{P}$  MRS of the brain and their use in evaluating optic pathway gliomas in children. *Eur J Radiol* 2014; 83 (2): 106–112.

8. **Law M.** Advanced imaging techniques in brain tumors. *Cancer Imaging*. 2009; 9: 4–9.
9. **Maintz D, Heindel W, Kugel H, Jaeger R, Lackner KJ.** Phosphorus-31 MR spectroscopy of normal adult human brain and brain tumours. *NMR Biomed* 2002; 15 (1): 18–27.
10. **Naressi A, Couturier C, Castang I, de Beer R, Graveron-Demilly D.** Java-based graphical user interface for MRUI, a software package for quantitation of in vivo/medical magnetic resonance spectroscopy signals. *Comput Biol Med* 2001; 31 (4): 269–286.
11. **Zhang X, Lin Y, Gillies RJ.** Tumor pH and Its Measurement. *J Nucl Med* 2010; 51 (8): 1167–1170.
12. **Hnilicová P, Richterová R, Kantorová E, Bittšanský M, Baranovičová E, Dobrota D.** Proton MR spectroscopic imaging of human glioblastomas at 1.5Tesla. *Gen Physiol Biophys* 2017; 36: 531–537.
13. **Hsu PP, Sabatini DM.** Cancer Cell Metabolism: Warburg and Beyond. *Cell* 2008; 134: 703–707.
14. **Marie SK, Shino SM.** Metabolism and brain cancer. *Clin* 2011; 66 (1): 33–43.
15. **Delikatny EJ, Chawla S, Leung DJ, Poptani H.** MR-Visible Lipids and the Tumor Microenvironment. *NMR Biomed* 2011; 24 (6): 592–611.
16. **Puri BK, Treasaden IH, Treasaden IH.** Neuroimaging-Methods. InTech; Chapter 10, The Use of 31-Phosphorus Magnetic Resonance Spectroscopy to Study Brain Cell Membrane Motion- Restricted Phospholipids 2012; 205–216.
17. **van der Kemp WJM, Klomp DWJ, Wijnen JP.** 31P T2s of Phosphomonoesters, Phosphodiesteres, and Inorganic Phosphate in the Human Brain at 7T. *Magnetic Resonance in Medicine*. 2018; 80: 29–35.
18. **Chawla S, Kim S, Loevner LA.** Proton and Phosphorous MR Spectroscopy in Squamous Cell Carcinomas of the Head and Neck. *Acad Radiol* 2009; 16 (11): 1366–1372.
19. **Du F, Zhu XH, Zhang Y et al.** Tightly coupled brain activity and cerebral ATP metabolic rate. *Proc Natl Acad Sci USA* 2008; 105 (17): 6409–6414.
20. **Zhu XH, Qiao H, Du F et al.** Quantitative imaging of energy expenditure in human brain. In: *NeuroImage* 2012; 60 (4): 2107–2117.
21. **de Souza AC, Justo GZ, de Araújo DR, Cavagis AD.** Defining the Molecular Basis of Tumor Metabolism: a Continuing Challenge Since Warburg's Discovery. *Cell Physiol Biochem* 2011; 28 (5): 771–792.
22. **Belouche-Babari M, Chung YL, Al-Saffar NMS, Falck-Miniotis M, Leach MO.** Metabolic assessment of the action of targeted cancer therapeutics using magnetic resonance spectroscopy. *Brit J Cancer* 2010; 102 (1): 1–7.
23. **DeBerardinis RJ, Lum JJ, Hatzivassiliou G, Thompson CB.** The Biology of Cancer: Metabolic Reprogramming Fuels Cell Growth and Proliferation. *Cell Metab* 2008; 7 (1): 11–20.
24. **Cichočka M.** Possibilities of phosphorous magnetic resonance spectroscopy (31P MRS) in brain diagnostics. *Acta Bio-Optica Inform Med Inzyn Biomed* 2017; 23 (4): 246–252.
25. **Heiss WD, Heindel W, Herholz K et al.** Positron Emission Tomography of fluorine-18-Deoxyglucose and Image-Guided Phosphorus 31 Magnetic Resonance Spectroscopy in Brain Tumors. *J Nucl Med* 1990; 31 (3): 302–310.
26. **Cheng XF, Wu RH.** Diagnostic Techniques and Surgical Management of Brain Tumors. China: InTech, Chapter 15, MR-Based Methods for pH Measurement in Brain Tumors: Current Status and Clinical Potential 2011; 288–302.

Received February 17, 2020.

Accepted March 26, 2020.